

This work was written as part of one of the author's official duties as an Employee of the United States Government and is therefore a work of the United States Government. In accordance with 17 U.S.C. 105, no copyright protection is available for such works under U.S. Law.

Public Domain Mark 1.0

<https://creativecommons.org/publicdomain/mark/1.0/>

Access to this work was provided by the University of Maryland, Baltimore County (UMBC) ScholarWorks@UMBC digital repository on the Maryland Shared Open Access (MD-SOAR) platform.

Please provide feedback

Please support the ScholarWorks@UMBC repository by emailing scholarworks-group@umbc.edu and telling us what having access to this work means to you and why it's important to you. Thank you.



Advanced angular interpolation in the vector radiative transfer for coupled atmosphere and ocean systems

Peng-Wang Zhai^{a,*}, Yongxiang Hu^b, Damien B. Josset^a, Charles R. Trepte^b, Patricia L. Lucker^a, Bing Lin^b

^a SSAI, MS 475 NASA Langley Research Center, Hampton, VA 23681, USA

^b MS 475 NASA Langley Research Center, Hampton, VA 23681, USA

ARTICLE INFO

Article history:

Received 29 June 2012

Received in revised form

27 September 2012

Accepted 29 September 2012

Available online 9 October 2012

Keywords:

Atmospheric and ocean optics

Radiative transfer

Polarization

ABSTRACT

We apply the iteration of source function (IOSF) philosophy to the successive order of scattering method for solving the vector radiative transfer equation in the coupled atmosphere and ocean system. A major class of radiative transfer solvers only provides the radiation field at discrete viewing zenith angles. The radiation field at other angles is found by interpolation. The iteration of source matrix method integrates the product of the radiation field and source matrix at quadrature points to obtain the radiation field at arbitrary viewing angles. The resultant solution includes the radiation contributions from all scattering orders higher than one. The analytical single scattering solution is then added to find the total radiation field. The proposed scheme includes the benefits of both the IOSF interpolation and the analytical single scattering solution. Boundary conditions for a flat air–sea interface are fully considered. A test case of a coupled atmosphere and ocean system shows that this combined method improves the polarized radiation field greatly in comparison with the regular polynomial interpolation method.

© 2012 Elsevier Ltd. All rights reserved.

1. Introduction

Radiative transfer equation governs the radiation field in turbid media which scatters, absorbs, and emits radiation [1–3]. Radiative transfer has important applications in astrophysics, atmospheric and ocean optics, remote sensing, Earth climate, and many other research disciplines [4,5]. The analytical solution of the radiative transfer equation only exists for a few ideal cases, such as isotropic and Rayleigh scattering in an one-dimensional medium [1]. For more general cases people rely on numerical methods to find and analyze solutions to the radiative transfer equation. Among these methods, the Monte Carlo method solves radiative transfer stochastically, i.e., pseudo-random numbers are

used to decide the occurrence of a scattering event, the scattering angle, the magnitude of the detector signals, and many other aspects of the physical process [6]. The biasing techniques for the Monte Carlo method can be used to estimate the radiance at arbitrary viewing angles [7]. Nearly all other methods represent the radiation field at discrete angles. Gaussian or other quadrature schemes are then used to perform angular integration involved in the radiative transfer equation. An incomplete list of these methods is included in the reference section [8–18]. These methods all rely on interpolation schemes in order to get the radiance or Stokes parameters at arbitrarily desired angles.

Classical interpolation schemes include polynomial, rational, or cubic spline interpolation [19]. However, these methods are not reliable and accurate when the radiation field is discontinuous or changes rapidly. One example will be the downwelling radiation field in the ocean where the well-known Fresnel cone is present. The Fresnel cone is a

* Corresponding author. Tel.: +1 757 864 6288.

E-mail address: pengwang.zhai-1@nasa.gov (P.-W. Zhai).

bright region due to the atmospheric light transmitted in the water. Outside the Fresnel cone is a dark region in which only multiple scattered light exists. In this and other similar cases a regular interpolation scheme could not produce an acceptable radiation field. The DIScrete Ordinate Radiative Transfer (DISORT) code [8] utilizes the iteration of source function method, which obtains the radiance at arbitrary viewing angles by integrating the source function as part of the post-processing procedure. Because of this, Schulz et al. [20] named it the post-processing of source function method in the Vector DIScrete Ordinate Radiative Transfer (VDISORT) code. Yan and Stamnes published the application of the scalar version (radiance only) of this method in the Coupled Atmosphere and Ocean System (CAOS) [21]. Hereafter this method is referred to as the Iteration of Source Matrix (IOSM) method because our focus is on the polarized radiation field in which the source matrix instead of source function is involved. The IOSM method is rooted in the radiative transfer theory and can handle extrapolations and sometimes even improve the discrete ordinate results [20]. Another way of predicting radiance at arbitrary angles is used in the matrix operator method [17], which supplements the Gaussian quadrature integration points with additional viewing zenith angles μ and assigns the integration weights of zero to these μ angles. Though the implementations are largely different for the two methods, the physical meaning behind these two methods is similar to the source matrix iteration formulations discussed by Dave [22].

It is also possible to implement the IOSM method in other radiative transfer schemes. Min and Duan [13] report that the method is implemented in their successive order of scattering (SOS) code for vector radiative transfer in atmosphere. Ota et al. [23] implemented the IOSM method in a hybrid discrete ordinate–matrix operator method for the CAOS. In this paper, we report the detailed formulas for applying the IOSM method to the vector radiative transfer solution for the CAOS in the SOS code [24,25]. The physical analysis shows that the direct application of the IOSM yields the radiation field with the first order scattering not included. The analytical single scattering solution [26–28] of the radiation field for the CAOS is then added to form a unified solution to the vector radiative transfer equation. The boundary conditions of the radiation field across a flat air–sea interface in the CAOS are taken into account.

Ota et al. [23] also apply both the IOSM and single scattering correction in their implementation. The formulation presented in this work is characterized by: (1) our formulas are based on the SOS method; (2) our method does not subtract the single scattering solution due to truncated phase matrix from the overall solution because the integration of source matrix automatically excludes the first order scattering solution; (3) in our implementation the boundary conditions work together with the IOSM radiation field, while Ota et al. use boundary conditions to replace the IOSM radiation field due to the different nature of the radiative transfer solvers; and 4. our analytical single scattering solution includes the scattered light of the sun glint [28]. This

paper is organized as follows: Section 2 introduces the theoretical foundations for using the unified IOSM and single scattering method in the SOS code; Section 3 describes numerical simulation results and discussions; and Section 4 presents the conclusions.

2. Theory

An attractive feature of the IOSM method is that it is a post-processing procedure. In other words, it does not change the main structure or formulas of the radiative transfer solvers and is implemented after the solution at Gaussian quadrature points are obtained [20]. Similarly, we assume here that the Fourier components of the Stokes parameters at Gaussian quadrature points and at discrete optical depth levels are obtained by the SOS method in Zhai et al. [24,25]. The polarized radiation field, i.e., the Stokes parameters, is denoted as $\mathbf{L} = (I, Q, U, V)^T$, where T stands for the transpose of the vector. As a part of the standard mathematical manipulation, the Stokes parameters \mathbf{L} and phase matrices \mathbf{P} are expanded into Fourier series to transform viewing azimuth angle dependence into Fourier expansion order (see Eqs. (9) and (10) in Zhai et al. [24]). Recall that $\mathbf{L}_n^m = (I_{n,\cos}^m, Q_{n,\cos}^m, U_{n,\sin}^m, V_{n,\sin}^m)^T$, where n is the order of scattering; m is the order of Fourier decomposition; cos and sin are used to denote the cosine and sine components of the radiation field, respectively. In addition, the phase matrix with Fourier expansion order of m is $\mathbf{P}^m = \mathbf{P}_{\cos}^m + \mathbf{P}_{\sin}^m \mathbf{D}$ with $\mathbf{D} = \text{diag}\{1, 1, -1, -1\}$. With these definitions, the quantity

$$\mathbf{L}^m(\tau_k, \mu_p) = \sum_{n=1}^N \mathbf{L}_n^m(\tau_k, \mu_p), \quad (1)$$

is known, where τ_k is the discrete optical depth level where the radiation field is evaluated; μ_p is the cosine of the viewing zenith angle at Gaussian quadrature point p ; and N is the maximum order of scattering being evaluated. In this paper the cosine of the zenith angle μ_p or μ larger than 0 means upwelling directions and vice versa. In the following derivations it should be understood that \mathbf{L}^m is the total diffuse radiation field, which does not include the direct solar light contribution. If the scattering medium is a CAOS, \mathbf{L}^m does not include the sun glint.

The source matrix at an arbitrary angle μ (different from quadrature points) due to all orders of scattering is the angular integration of the phase matrix and radiance vector production (see Eq. (12c) in Zhai et al. [24]):

$$\begin{aligned} \mathbf{S}^m(\tau_k, \mu) &= \frac{\omega(\tau_k)}{2} \int_{-1}^1 \mathbf{P}^m(\tau_k, \mu, \mu') \cdot \mathbf{L}^m(\tau_k, \mu') d\mu' \\ &= \frac{\omega(\tau_k)}{2} \sum_{p=1}^{N_G} w_p \mathbf{P}^m(\tau_k, \mu, \mu_p) \cdot \mathbf{L}^m(\tau_k, \mu_p), \end{aligned} \quad (2)$$

where $\omega(\tau_k)$ is the single scattering albedo at optical depth τ_k ; N_G is the total number of Gaussian quadrature points, either in the atmosphere or in the ocean; and w_p is the integration weight associated with the quadrature point p . In the standard SOS solution, the phase matrix \mathbf{P}^m is only needed at the Gaussian quadrature points (μ_q, μ_p) . In this effort of finding the Stokes parameters at arbitrary angle μ , we also need $\mathbf{P}^m(\tau_k, \mu, \mu_p)$ as suggested in Eq. (2).

This is easily achieved by expanding the phase matrix Fourier components in terms of the Wigner d coefficients (see Eq. (A.13) in Ref. [24], also Ref. [29–31]). Careful examination of the SOS formulations shows that the scattering order of the source matrix at the left-hand side in Eq. (2) is always one order of scattering higher than the order of the radiation field at the right-hand side. Since $\mathbf{L}^m(\tau_k, \mu_p)$ is the total diffuse field that includes all orders of scattering, \mathbf{S}^m in Eq. (2) will be the source matrix for all orders of scattering higher than one.

The Fourier components of the Stokes parameters at the viewing zenith angle of μ are then obtained through optical depth integration of the source matrix:

$$\begin{aligned} \mathbf{L}^m(\tau_k, \mu < 0) &= - \int_{\tau_l}^{\tau_k} e^{-(\tau' - \tau_k)/\mu} \mathbf{S}^m(\tau', \mu) d\tau' / \mu \\ &= e^{\delta\tau/\mu} \mathbf{L}^m(\tau_{k-1}, \mu < 0) - \int_{\tau_{k-1}}^{\tau_k} e^{-(\tau' - \tau_k)/\mu} \mathbf{S}^m(\tau', \mu) d\tau' / \mu, \end{aligned} \quad (3)$$

$$\begin{aligned} \mathbf{L}^m(\tau_k, \mu > 0) &= \int_{\tau_k}^{\tau_u} e^{-(\tau' - \tau_k)/\mu} \mathbf{S}^m(\tau', \mu) d\tau' / \mu \\ &= e^{-\delta\tau/\mu} \mathbf{L}^m(\tau_{k+1}, \mu > 0) + \int_{\tau_k}^{\tau_{k+1}} e^{-(\tau' - \tau_k)/\mu} \mathbf{S}^m(\tau', \mu) d\tau' / \mu, \end{aligned} \quad (4)$$

where $\delta\tau$ is the optical depth thickness between successive vertical layers; τ_l and τ_u are the lower and upper optical depth boundary of the medium in consideration, respectively. In atmosphere $\tau_l = 0$ and $\tau_u = \tau_a^*$ are the optical depths at the top and bottom of the atmosphere, respectively; in ocean $\tau_l = \tau_o$ and $\tau_u = \tau_o^*$ are the optical depths at the top and bottom of the ocean, respectively. The superscript $*$ is used to denote the bottom of either the atmosphere or ocean. Note that $\tau_o = \tau_a + \epsilon$ where ϵ is an infinitesimal. As in Refs. [24,25], the optical depth integration in Eqs. (3) and (4) is evaluated using the exponential-linear approximation [32]. To initialize the iteration integration in Eqs. (3) and (4), $\mathbf{L}^m(\tau_l, \mu < 0) = 0$ and $\mathbf{L}^m(\tau_u, \mu > 0) = 0$ are used.

The radiation field $\mathbf{L}^m(\tau_k, \mu)$ in Eqs. (3) and (4) includes the contributions from all orders of scattering higher than one, a consequence of the presence of \mathbf{S}^m defined by Eq. (2). To make up the missing contribution from the first order of scattering, one could use the single scattering solution due to the truncated phase matrix (see Eqs. (12a) and (12b) in Zhai et al. [24]). However, it is more attractive to use the exact single scattering solution [26–28] in which no truncation techniques [33,34] are involved. The single scattering solution for the CAOS shown in Zhai et al. [28] is the explicit function of azimuth angle ϕ , i.e., no Fourier expansion is used. To obtain the total radiation field, we first convert $\mathbf{L}^m(\tau_k, \mu)$ into the azimuth angle domain:

$$\begin{aligned} \mathbf{L}'(\tau_k, \mu, \phi) &= \sum_{m=0}^M (2 - \delta_{0m}) \{ \cos[m(\phi - \phi_0)] \mathbf{L}_{\cos}^m(\tau_k, \mu) \\ &\quad + \sin[m(\phi - \phi_0)] \mathbf{L}_{\sin}^m(\tau_k, \mu) \}, \end{aligned} \quad (5)$$

where ϕ and ϕ_0 are the viewing and solar azimuth angles, respectively; M is the maximum Fourier expansion order; \mathbf{L}_{\cos}^m and \mathbf{L}_{\sin}^m are the cosine and sine components of \mathbf{L}^m as

in Eqs. (3) and (4). Then the total radiation field is obtained by adding the single scattering contribution to $\mathbf{L}'(\tau_k, \mu, \phi)$. It is necessary to discuss two different scenarios separately to avoid confusion. These two scenarios are: (i) an atmosphere bounded by a lambertian land surface; and (ii) a coupled atmosphere and ocean system with a flat ocean surface and a lambertian ocean bottom. Another important scenario is the same as (ii) but with a rough ocean surface. In this case the sun glint has an angular distribution due to the bidirectional nature of the reflection or transmission matrix of the rough interface. Consequently, the calculation of the scattering of the sun glint using exact original phase matrix will involve time-consuming double fold angular integrations (over zenith and azimuth angles) for each of the desired viewing angle. Preliminary tests show that this is computationally too costly. For efficiency, the current implementation uses regular polynomial interpolation for the scattered light from the sun glint in the case of rough interface. The final radiation field is a mixture of regular interpolation and IOSM method. The details of that implementation of the rough ocean surface case are excluded in the following part of this paper.

2.1. Atmosphere bounded by a lambertian land surface

In this case the total radiation field is the summation of three terms: $\mathbf{L}'(\tau_k, \mu, \phi)$, single scattering contribution from direct solar lights, and the contribution from surface reflection. The analytical single scattering solution induced by the direct solar light is [26–28]:

$$\begin{aligned} \mathbf{L}'_1(\tau_k, \mu < 0, \phi) &= \mathbf{L}'_1(\tau_{k-1}, \mu < 0, \phi) \exp\left(-\frac{\tau_{k-1} - \tau_k}{\mu}\right) \\ &\quad + \frac{\omega(\tau_k) - \mu_0}{4\pi \mu - \mu_0} \cdot \left[\exp\left(\frac{\tau_k}{\mu_0}\right) - \exp\left(\frac{\tau_{k-1} - \tau_k}{\mu_0} - \frac{\tau_{k-1} - \tau_k}{\mu}\right) \right] \\ &\quad \times \mathbf{P}(\tau_k, \mu, \phi, \mu_0, \phi_0) \cdot \mathbf{E}_0, \end{aligned} \quad (6)$$

$$\begin{aligned} \mathbf{L}'_1(\tau_k, \mu > 0, \phi) &= \mathbf{L}'_1(\tau_{k+1}, \mu > 0, \phi) \exp\left(-\frac{\tau_{k+1} - \tau_k}{\mu}\right) \\ &\quad + \frac{\omega(\tau_k) - \mu_0}{4\pi \mu - \mu_0} \cdot \left[\exp\left(\frac{\tau_k}{\mu_0}\right) - \exp\left(-\frac{\tau_{k+1} - \tau_k}{\mu} + \frac{\tau_{k+1}}{\mu_0}\right) \right] \\ &\quad \times \mathbf{P}(\tau_k, \mu, \phi, \mu_0, \phi_0) \cdot \mathbf{E}_0, \end{aligned} \quad (7)$$

with $\mathbf{L}'_1(\tau = 0, \mu < 0, \phi) = 0$ and $\mathbf{L}'_1(\tau_a^*, \mu > 0, \phi) = 0$ understood in the recursive relation. \mathbf{E}_0 is the solar irradiance at the Top of the Atmosphere (TOA). Note that the phase matrix $\mathbf{P}(\tau_k, \mu, \phi, \mu_0, \phi_0) = \mathbf{R}(\pi - i_2) \cdot \mathbf{F}(\tau_k, \Theta) \cdot \mathbf{R}(-i_1)$ [24], where \mathbf{R} is the rotation matrix; i_1 and i_2 are the rotation angles before and after the scattering event, respectively; \mathbf{F} is the single scattering matrix; and Θ is the scattering angle. The cosine of the solar zenith angle $\mu_0 = \cos \theta_0 < 0$ because $\theta_0 > 90^\circ$ and the solar zenith angle is defined as the angle between the incident solar light propagation direction and the local zenith. Eq. (6) has a singularity at $\mu = \mu_0$. In this case the solution reduces to:

$$\begin{aligned} \mathbf{L}'_1(\tau_k, \mu_0, \phi_0) &= \mathbf{L}'_1(\tau_{k-1}, \mu_0, \phi_0) \exp\left(-\frac{\tau_{k-1} - \tau_k}{\mu_0}\right) \\ &\quad + \frac{\omega(\tau_k)}{4\pi} \exp\left(\frac{\tau_k}{\mu_0}\right) \frac{\tau_k - \tau_{k-1}}{-\mu_0} \mathbf{P}(\tau_k, \mu_0, \phi_0, \mu_0, \phi_0) \cdot \mathbf{E}_0. \end{aligned} \quad (8)$$

The total polarized radiation field in the atmosphere is then:

$$\mathbf{L}(\tau_k, \mu < 0, \phi) = \mathbf{L}'(\tau_k, \mu < 0, \phi) + \mathbf{L}_1'(\tau_k, \mu < 0, \phi), \quad (9a)$$

$$\mathbf{L}(\tau_k, \mu > 0, \phi) = \mathbf{L}'(\tau_k, \mu > 0, \phi) + \mathbf{L}_1'(\tau_k, \mu > 0, \phi) + \frac{\omega_g}{\pi} F_a \exp\left(-\frac{\tau_a^* - \tau_k}{\mu}\right), \quad (9b)$$

where ω_g is the reflection albedo of the lambertian ground surface; F_a is the total downwelling irradiance at the ground obtained from the SOS solution as in Refs. [24,25]. The third term in Eq. (9b) is needed because \mathbf{L}_1' accounts for the single scatter solution but not for the surface reflection of the diffuse light. Eqs. (9a) and (9b) also exclude the error introduced from truncation schemes like delta-M [33] or δ fit methods [34] for the single scattering contribution by using the exact original phase matrix.

2.2. Coupled atmosphere and ocean systems with a flat surface

As it is stressed earlier, the term \mathbf{L}^m does not include the sun glint. Therefore, $\mathbf{L}'(\tau_k, \mu, \phi)$ does not include the scattered light induced by the sun glint. In addition, the reflection and transmission of the diffuse light across the interface has to be accounted for. In the atmosphere, the exact solution of the diffuse light induced by the sun glint is [28]

$$\begin{aligned} \mathbf{L}_1'(\tau_k, \mu < 0, \phi) &= \mathbf{L}_1''(\tau_{k-1}, \mu < 0, \phi) \exp\left(-\frac{\tau_{k-1} - \tau_k}{\mu}\right) \\ &+ \frac{\omega(\tau_k)}{4\pi} \frac{\mu_0}{\mu + \mu_0} \exp\left(\frac{2\tau_a^* - \tau_k}{\mu_0}\right) \\ &\times \left\{ 1 - \exp\left[-(\tau_{k-1} - \tau_k) \left(\frac{1}{\mu_0} + \frac{1}{\mu}\right)\right] \right\} \\ &\times \mathbf{P}(\tau_k, \mu, \phi, -\mu_0, \phi_0) \cdot \mathbf{r}(\pi - \theta_0) \cdot \mathbf{E}_0, \end{aligned} \quad (10)$$

$$\begin{aligned} \mathbf{L}_1''(\tau_k, \mu > 0, \phi) &= \mathbf{L}_1''(\tau_{k+1}, \mu > 0, \phi) \exp\left(-\frac{\tau_{k+1} - \tau_k}{\mu}\right) \\ &+ \frac{\omega(\tau_k)}{4\pi} \frac{-\mu_0}{\mu + \mu_0} \exp\left(\frac{2\tau_a^* - \tau_k}{\mu_0}\right) \\ &\times \left\{ \exp\left[-(\tau_{k+1} - \tau_k) \left(\frac{1}{\mu} + \frac{1}{\mu_0}\right)\right] - 1 \right\} \\ &\times \mathbf{P}(\tau_k, \mu, \phi, -\mu_0, \phi_0) \mathbf{r}(\pi - \theta_0) \cdot \mathbf{E}_0. \end{aligned} \quad (11)$$

In case of $\mu + \mu_0 = 0$, $\mathbf{L}_1''(\tau_k, \mu > 0, \phi)$ reduces to the form of:

$$\begin{aligned} \mathbf{L}_1''(\tau_k, -\mu_0, \phi_0) &= \mathbf{L}_1''(\tau_{k+1}, -\mu_0, \phi_0) \exp\left(\frac{\tau_{k+1} - \tau_k}{\mu_0}\right) \\ &+ \frac{\omega(\tau_k)}{4\pi} \frac{\tau_{k+1} - \tau_k}{-\mu_0} \exp\left(\frac{2\tau_a^* - \tau_k}{\mu_0}\right) \\ &\times \mathbf{P}(\tau_k, -\mu_0, \phi_0, -\mu_0, \phi_0) \mathbf{r}(\pi - \theta_0) \cdot \mathbf{E}_0. \end{aligned} \quad (12)$$

The initial conditions for these recursive relations are again: $\mathbf{L}_1''(0, \mu < 0, \phi) = 0$ and $\mathbf{L}_1''(\tau_a^*, \mu > 0, \phi) = 0$. The Fresnel reflection matrix \mathbf{r} and the transmission matrix \mathbf{t} below are given by Eqs. (47) and (48) in Zhai et al. [25].

In the ocean, the diffuse light originating from the direct sun light transmitted through the flat ocean

surface is [28]:

$$\begin{aligned} \mathbf{L}_1^o(\tau_k, \mu < 0, \phi) &= \mathbf{L}_1^o(\tau_{k-1}, \mu < 0, \phi) \exp\left(-\frac{\tau_{k-1} - \tau_k}{\mu}\right) \\ &+ \frac{\omega(\tau_k)}{4\pi} \frac{-\mu_0}{\mu - \mu'_0} \exp\left(\frac{\tau_a^*}{\mu_0}\right) \\ &\cdot \left[\exp\left(\frac{\tau_k - \tau_o}{\mu'_0}\right) - \exp\left(\frac{\tau_{k-1} - \tau_o}{\mu'_0} - \frac{\tau_{k-1} - \tau_k}{\mu}\right) \right] \\ &\cdot \mathbf{P}(\tau, \mu, \phi, \mu'_0, \phi_0) \cdot \mathbf{t}(\pi - \theta_0) \cdot \mathbf{E}_0, \end{aligned} \quad (13)$$

$$\begin{aligned} \mathbf{L}_1^o(\tau_k, \mu'_0, \phi_0) &= \mathbf{L}_1^o(\tau_{k-1}, \mu'_0, \phi_0) \exp\left(-\frac{\tau_{k-1} - \tau_k}{\mu'_0}\right) \\ &+ \frac{\omega(\tau_k)}{4\pi} \frac{|\mu_0|}{|\mu'_0|} \exp\left(\frac{\tau_a^*}{\mu_0}\right) \frac{\tau_{k-1} - \tau_k}{|\mu'_0|} \mathbf{P}(\tau, \mu'_0, \phi_0, \mu'_0, \phi_0) \\ &\cdot \mathbf{t}(\pi - \theta_0) \cdot \mathbf{E}_0, \end{aligned} \quad (14)$$

$$\begin{aligned} \mathbf{L}_1^o(\tau_k, \mu > 0, \phi) &= \mathbf{L}_1^o(\tau_{k+1}, \mu > 0, \phi) \exp\left(-\frac{\tau_{k+1} - \tau_k}{\mu}\right) \\ &+ \frac{\omega(\tau_k)}{4\pi} \frac{-\mu_0}{\mu - \mu'_0} \exp\left(\frac{\tau_a^*}{\mu_0}\right) \\ &\cdot \left[\exp\left(\frac{\tau_k - \tau_o}{\mu'_0}\right) - \exp\left(\frac{\tau_{k+1} - \tau_o}{\mu'_0} - \frac{\tau_{k+1} - \tau_k}{\mu}\right) \right] \\ &\cdot \mathbf{P}(\tau, \mu, \phi, \mu'_0, \phi_0) \cdot \mathbf{t}(\pi - \theta_0) \cdot \mathbf{E}_0. \end{aligned} \quad (15)$$

In the above equations, $\mu'_0 = \cos \theta'_0$ and $\sin \theta_0 = n_w \sin \theta'_0$, where n_w is the index of refraction for ocean water. Eqs. (10)–(15) were reported in Zhai et al. [28] and reproduced here with notations consistent with this paper.

With the single scattering solution given, the total downwelling radiation field at arbitrary viewing zenith angle μ in the atmosphere is

$$\begin{aligned} \mathbf{L}_a(\tau_k, \mu < 0, \phi) &= \mathbf{L}'(\tau_k, \mu < 0, \phi) \\ &+ \mathbf{L}_1'(\tau_k, \mu < 0, \phi) + \mathbf{L}_1''(\tau_k, \mu < 0, \phi), \end{aligned} \quad (16)$$

where the subscript a is used to discriminate from the radiation field in Eq. (9). The upwelling radiation in the atmosphere or downwelling radiation in ocean has to include the reflection from and transmission through the ocean surface. The upwelling radiation field in the ocean is

$$\begin{aligned} \mathbf{L}_o(\tau_k, \mu > 0, \phi) &= \mathbf{L}'(\tau_k, \mu > 0, \phi) + \mathbf{L}_1^o(\tau_k, \mu > 0, \phi) \\ &+ \frac{\omega_b}{\pi} F_o \exp\left(-\frac{\tau_o^* - \tau_k}{\mu}\right), \end{aligned} \quad (17)$$

where ω_b is the ocean bottom reflection albedo and F_o is the downwelling irradiance at the ocean bottom obtained from the SOS solution similar to F_a . The upwelling radiation field in atmosphere is then:

$$\begin{aligned} \mathbf{L}_a(\tau_k, \mu > 0, \phi) &= \mathbf{L}'(\tau_k, \mu > 0, \phi) + \mathbf{L}_1'(\tau_k, \mu > 0, \phi) \\ &+ \mathbf{L}_1''(\tau_k, \mu > 0, \phi) + \left[\mathbf{r}(\theta) \cdot \mathbf{L}_a(\tau_a^*, -\mu, \phi) + \frac{\mathbf{t}(\theta') \cdot \mathbf{L}_o(\tau_o, \mu', \phi)}{n_w^2} \right] \\ &\times \exp\left(-\frac{\tau_a^* - \tau_k}{\mu}\right), \end{aligned} \quad (18)$$

where $\theta = \arccos \mu$; $\mu' = \cos \theta'$, and $\sin \theta = n_w \sin \theta'$. The downwelling radiation field in ocean is then:

$$\begin{aligned} \mathbf{L}_o(\tau_k, \mu < 0, \phi) &= \mathbf{L}'(\tau_k, \mu < 0, \phi) + \mathbf{L}_1^o(\tau_k, \mu < 0, \phi) \\ &+ [\mathbf{r}(\pi - \theta) \cdot \mathbf{L}_o(\tau_o, -\mu, \phi) + \mathbf{t}(\pi - \theta') \cdot \mathbf{L}_a(\tau_a^*, \mu', \phi) \cdot n_w^2] \\ &\times \exp\left(-\frac{\tau_k - \tau_o}{\mu}\right), \end{aligned} \quad (19)$$

where θ and θ' are larger than $\pi/2$ because $\theta = \arccos \mu$ and $\mu < 0$.

3. Results and discussion

We have outlined how to apply the IOSM method in combining the analytical single scattering solution with the SOS vector radiative transfer code for the CAOS. To validate and test our implementation, we adopted the same test case shown in Zhai et al. [28]. The case is a CAOS with optical depth of 0.5 for both the atmosphere and ocean. The single scattering albedo is 0.99 which is also the same for both media. The scattering matrix for both the atmosphere and ocean is the $L=60$ model [35], which is calculated by light scattering by spherical particles with a gamma size distribution. The effective radius and variance are $1.05 \mu\text{m}$ and 0.07, respectively. The wavelength is $0.782 \mu\text{m}$ at which the index of refraction is 1.43. The ocean surface is flat with refractive index of 1.338. The ocean bottom is lambertian with a reflection albedo of 0.1. The solar zenith angle is 78.4630° . Though this case is rather simple and unrealistic, the radiation contribution from all parts of the system, including atmosphere, interface, ocean, and bottom are

equally important so that the different branches of the code could be well tested.

To study the error for different parameters used in the calculation, a benchmark needs to be established. We use two independent methods, the SOS and Monte Carlo (MC) [36] methods to calculate the radiation field at four locations: the Top of the Atmosphere (TOA), Bottom of the Atmosphere (BOA), Top of the Ocean (TOO), and Bottom of the Ocean (BOO) [28]. Note that the TOO is immediately below the water surface. A photon history of 5×10^6 for the MC method and $N_G=100$ in the atmosphere and $N_G=200$ in the ocean for the SOS method are used. The agreement between the two methods is better than 0.1% everywhere. This way the benchmark is set up with uncertainty smaller than 0.1%. The Stokes parameters for this test case at all four locations are published in Zhai et al. [28]. Then we decrease N_G for the SOS method to test the error of the Stokes parameters for three methods: (1) the regular four degree polynomial interpolation (PLNM); (2) the PLNM combined with the Single scattering Correction (SC) method shown in Zhai et al. [28] (hereafter referred to as “PLNM+SC”); and (3) the IOSM method combined with the Analytical Single Scattering (ASS) technique (refer to as “IOSM+ASS”).

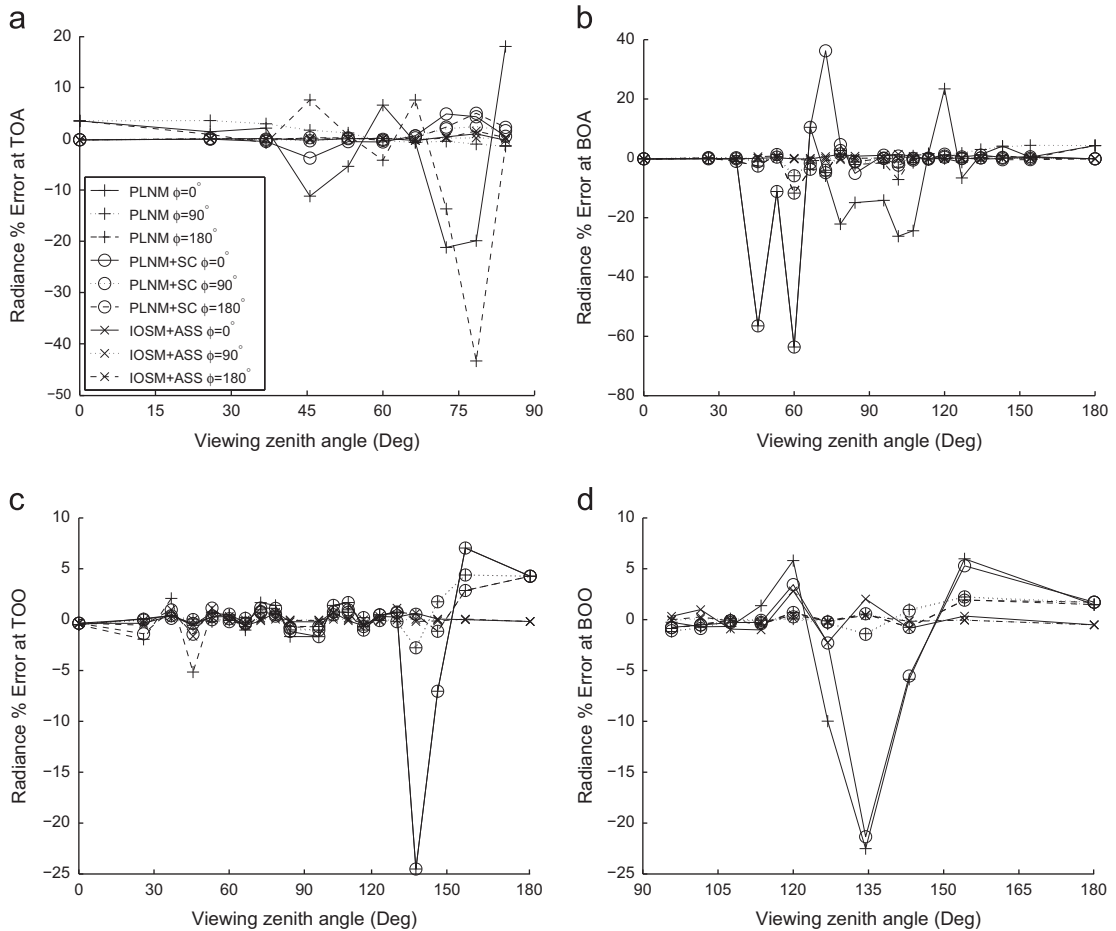


Fig. 1. Radiance percentage error at the four locations in the CAOS with $N_G=16$.

Fig. 1a–d show the radiance percentage error of the SOS code at the TOA, BOA, TOO, and BOO, respectively, as a function of the viewing zenith angle. The SOS results use $N_G=16$ and 32 for the atmosphere and ocean, respectively. The Delta-M method is used to truncate the phase matrix to maximum expansion order of $L=16$. The percentage error is defined as: $100 \times (I_{SOS} - I_{bench}) / I_{bench}$, where I_{bench} is the benchmark radiance calculated by the SOS method with $N_G=100$. Three viewing azimuth angles are shown: 0° , 90° , and 180° . The azimuth angle of the solar light propagation direction defines the azimuth angle of 0° (x -axis direction). The viewing zenith angle is measured by the angle between the viewing direction and the positive z -axis, which points to the local zenith. Y -axis is determined by the right handed x - y - z coordinate system. Therefore, $\theta = 0^\circ$ is looking at the Zenith, 180° is the nadir, and 90° points to the horizon. The viewing azimuth angle is defined by the angle between the projection of the viewing direction in the x - y plane and the positive x -direction. The figure legend used in Fig. 1a applies to all other figures in this paper.

At the TOA, the PLNM interpolation error could be as large as -45% at viewing zenith angles larger than 75° for the azimuth angle of 180° . The reason is that the radiance at the azimuth angle 180° shows a nonsmooth behavior from the zenith angle of 60° to 90° . We found that the

nonsmooth behavior of the radiance is caused by large oscillations of the scattering matrix at the backscattering direction. Also the Gaussian number $N_G=16$ does not provide data close enough to make an accurate interpolation. If the single scattering correction technique (PLNM+SC) is used, the error reduces to around 5% for those angles. With the IOSM+ASS technique described in this paper, the percentage error is smaller than 1% for all range of viewing angles. At the BOA, the largest error happens in the similar viewing zenith angle range as those at the TOA for the PLNM interpolation method due to similar radiance behavior. It is interesting to observe that the errors of the PLNM and PLNM+SC schemes are in similar range for upwelling radiances at BOA. This is because the single scattering solution for the upwelling radiance at the BOA is zero, so that single scattering correction does not make a difference. The difference between the two schemes at large viewing angles is resultant from the differences in the radiation field across the interface between the two schemes. The IOSM+ASS technique reduces the error to around 1% for all the viewing angles.

Similarly the errors from both the PLNM and PLNM+SC interpolation schemes are nearly equal to each other at the TOO for the downwelling radiance. The reason is again that the single scattering solution is zero for the downwelling

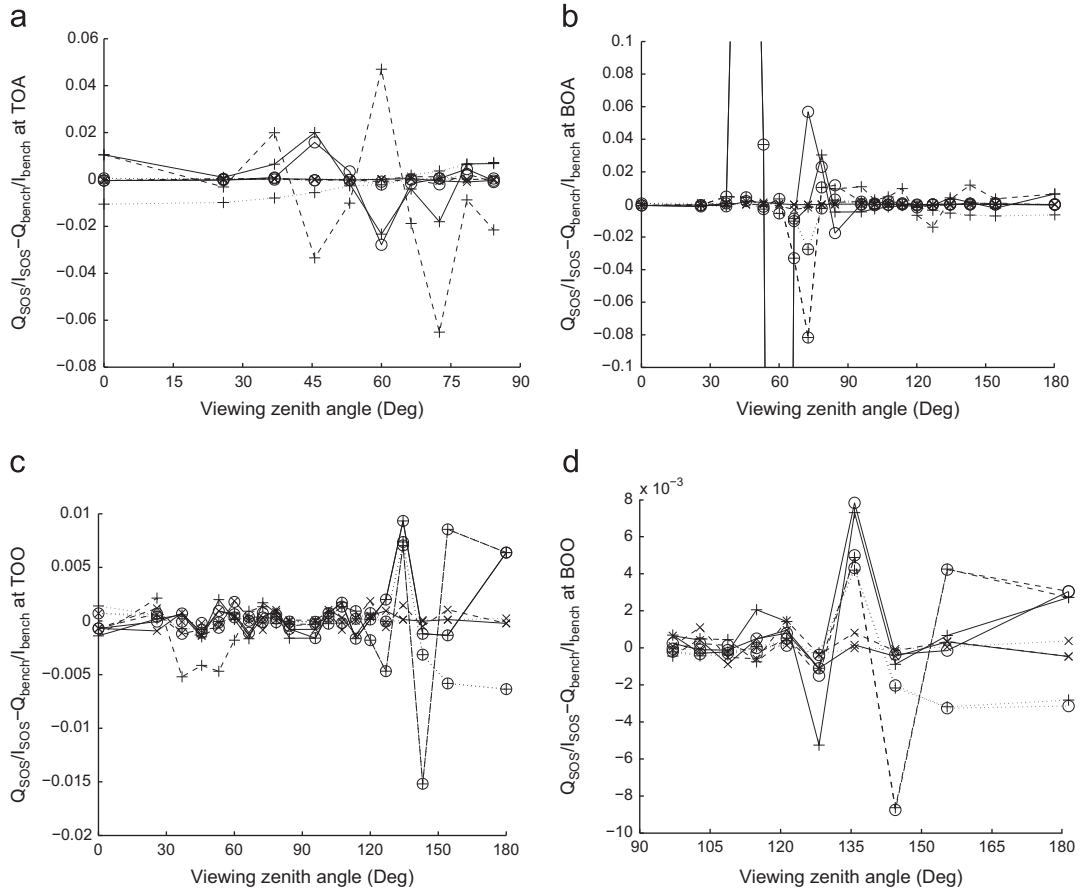


Fig. 2. Q/I error at the four locations in the CAOS with $N_G=16$.

radiance at the TOO. The IOSM+ASS method shows superior performance consistently. The largest percentage errors at the TOO and BOO occur around the critical viewing zenith angle of where the radiance has a discontinuity. The PLNM+SC does reduce the error for some of the angles but not always. The IOSM+ASS technique is indeed effective, which helps to reduce the error from 25% to a few percent in general.

To show the performance of the polarization calculation of the IOSM+ASS technique, Fig. 2a–d show the difference of Q/I calculated by the SOS method with $N_C=16$ and the benchmark results. In these figures the subscripts SOS and bench refer to the SOS results calculated with $N_C=16$ and $N_C=100$ in the atmosphere, respectively. Legends and symbols are the same as those in Fig. 1. The maximum error for the TOA is again at $\phi = 180^\circ$ and $\theta > 75^\circ$ due to the same reason explained in the plots of the radiance error. The PLNM error is as large as 0.06 and it is brought down to 0.02 by the single scattering correction. With the IOSM+ASS method, the error is even smaller (around 0.001). At the BOA the errors for the PLNM and PLNM+SC methods at $\phi = 0$ and $\theta = 60^\circ$ are exceptionally large (around 0.5) due to a polarization peak around this location. Readers are referred to Fig. 2 in Zhai et al. [28] for the plot of this

behavior. On the contrary, the error for the IOSM+ASS method is very small at the same location. The error scale ranges for Fig. 2b is from -0.1 to 0.1 in order to show the small error variation better. Consequently the large error of 0.5 at $\phi = 0^\circ$ and $\theta = 60^\circ$ for the PLNM and PLNM+SC is not shown in Fig. 2b. The error for PLNM at the BOA is prominent between 60° and 90° and single scattering correction does not reduce the error much because the single scattering solution for the upwelling radiance at the BOA is zero. With the IOSM+ASS method, the error lowers to the level of 0.002. For the TOO and BOO, the largest errors again occur around the critical angle of 131.6° . The error from PLNM+SC technique is largely the same as the simple PLNM method for the downwelling field at the TOO due to the zero single scattering contribution for downwelling radiance. The IOSM+ASS method shows a very small error everywhere which validates its reliability.

To complete the comparison, Figs. 3 and 4 show the errors of the Stokes parameters U/I and V/I , respectively. Only the results for $\phi = 90^\circ$ are shown because U/I and V/I are identically zero for $\phi = 0$ and $\phi = 180^\circ$. The PLNM+SC error is generally smaller than the PLNM method but not always, depends on how much the single scattering solution contributes to the total field. There are some

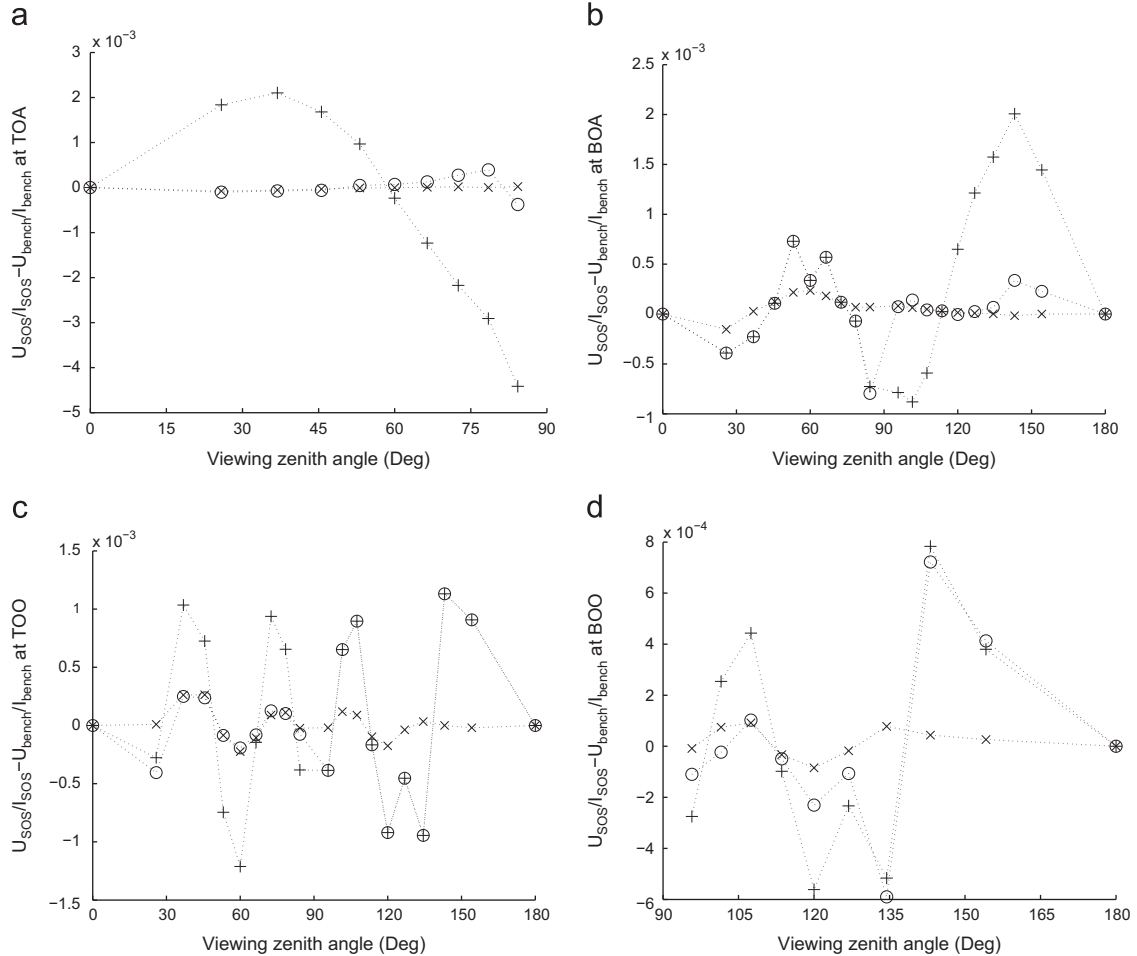


Fig. 3. U/I error at the four locations in the CAOS with $N_C=16$.

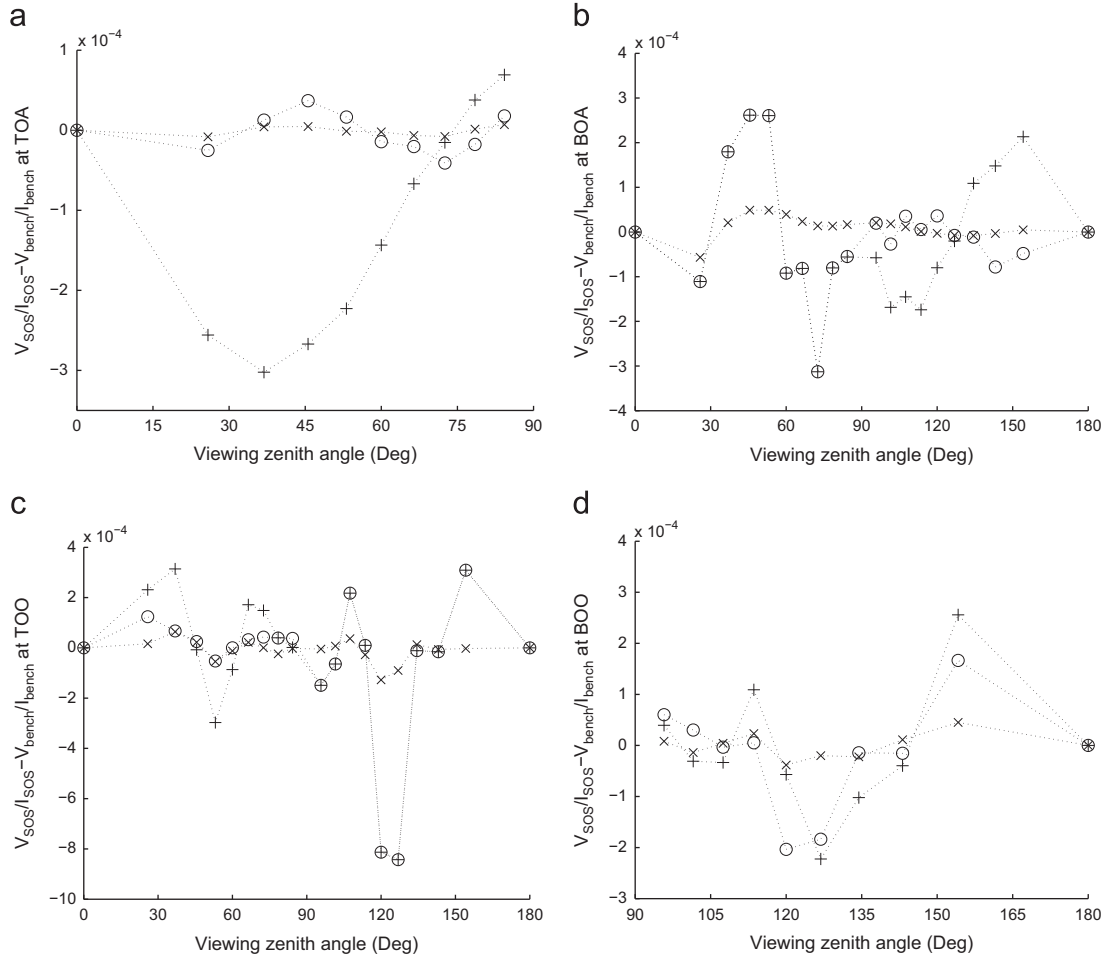


Fig. 4. V/I error at the four locations in the CAOS with $N_G=16$.

viewing angle regions where the PLNM+SC error is the same as the PLNM error. For example, the upwelling radiance field at the BOA and the downwelling radiance at the TOO, where the single scattering solution is zero. Similar to the radiance and Q errors, U/I and V/I comparisons show that the IOSM+ASS provides consistent and reliable performance at all viewing angles regardless of the smoothness of the radiance fields.

We have also tested the code with $N_G=30$ in the atmosphere. The IOSM+ASS method yields the largest relative error of 0.1% for the radiance, which shows that the IOSM+ASS converges fast to the true solutions. The IOSM combined with the analytical single scattering technique shows large improvement in the accuracy of the vector radiative transfer calculation. As emphasized in Schulz and Stamnes [20], this is a post-processing procedure which does not change the structure of the radiative transfer solver. The extra information needed is $\mathbf{P}^m(\tau, \mu, \mu_p)$ (see Eq. (2)) and the analytical single scattering solution shown in Zhai et al. [28] for a CAOS. For the case we tested, the IOSM+ASS post-processing scheme takes about 1/100 s which is only a small fraction of the total time consumed by the SOS radiative transfer calculation.

4. Conclusion

In this paper we report the application of the IOSM method for obtaining the polarized radiation field at arbitrary viewing angles for the CAOS with the SOS algorithm. In this method, the polarized radiation field at Gaussian quadrature angles together with the source matrix are integrated to obtain the radiation field at arbitrary viewing zenith angles. The resultant field includes the contributions from all scattering orders higher than one. The analytical single scattering solution is then added to the IOSM solution to achieve a complete solution. Boundary conditions at the atmosphere and ocean interface are fully taken into account. In order to validate the implementation, we used two independent radiative transfer solutions (the SOS and MC methods) with high quadrature or photon package numbers to achieve agreement better than 0.1% to establish a benchmark. Then, the SOS was re-run with lower quadrature numbers to test how the IOSM method combined with the analytical single scattering solution improves the polarized radiation field calculation. A test case shows that this scheme reduces the error from 50% down to a few per cent for $N_G=16$. The maximum error of the other Stokes parameters dropped

significantly. The IOSM method works well regardless of the smoothness of the radiation field. Very often the polarized radiation field shows discontinuities and non-smoothness in atmosphere and ocean optics, for example, see the case presented in [28]. The current technique would produce accurate and reliable results for these cases. The method presented in this paper therefore has important applications for the radiative transfer and remote sensing community.

Acknowledgments

This study is supported by the NASA Radiation Science program administrated Hal Maring and the Biogeochemistry program administrated by Paula Bontempi.

References

- [1] Chandrasekhar S. Radiative transfer. New York: Dover; 1960.
- [2] Preisendorfer RW. Radiative transfer on discrete spaces. Oxford: Pergamon Press; 1965.
- [3] Mishchenko MI, Travis LD, Lacis AA. Multiple scattering of light by particles. New York: Cambridge University Press; 2006.
- [4] Mobley CD. Light and water: radiative transfer in natural waters. San Diego: Academic Press; 1994.
- [5] Liou KN. An introduction to atmospheric radiation. 2nd ed. San Diego: Academic Press; 2002.
- [6] Kattawar GW, Plass GN. Degree and direction of polarization of multiple scattered light. 1: homogeneous cloud layers. Appl Opt 1972;11:2851–65.
- [7] Roberti L. Monte Carlo radiative transfer in the microwave and in the visible: biasing techniques. Appl Opt 1997;36:7929–38.
- [8] Stamnes K, Tsay SC, Wiscombe W, Jayaweera K. Numerically stable algorithm for discrete-ordinate method radiative transfer in multiple scattering and emitting layered media. Appl Opt 1988;27:2502–9.
- [9] Weng F. A multi-layer discrete-ordinate method for vector radiative transfer in a vertically-inhomogeneous, emitting and scattering atmosphere—I. theory. J Quant Spectrosc Radiat Transfer 1992;47:19–33.
- [10] Schulz FM, Stamnes K, Weng F. VDISORT: an improved and generalized discrete ordinate method for polarized vector radiative transfer. J Quant Spectrosc Radiat Transfer 1999;61:105–22.
- [11] Mishchenko MI. Reflection of polarized light by plane-parallel slabs containing randomly-oriented, nonspherical particles. J Quant Spectrosc Radiat Transfer 1991;46:171–81.
- [12] Garcia RDM, Siewert CE. The F_N method for radiative transfer models that include polarization effects. J Quant Spectrosc Radiat Transfer 1989;41:117–45.
- [13] Min Q, Duan M. A successive order of scattering model for solving vector radiative transfer in the atmosphere. J Quant Spectrosc Radiat Transfer 2004;87:243–59.
- [14] Lenoble J, Herman M, Deuzé JL, Lafrance B, Santer R, Tanré D. A successive order of scattering code for solving the vector equation of transfer in the earths atmosphere with aerosols. J Quant Spectrosc Radiat Transfer 2007;107:479–507.
- [15] Chami M, Santer R, Dilligeard E. Radiative transfer model for the computation of radiance and polarization in an ocean-atmosphere system: polarization properties of suspended matter for remote sensing. Appl Opt 2001;40:2398–416.
- [16] Evans KF. The spherical harmonic discrete ordinate method for three-dimensional atmospheric radiative transfer. J Atmos Sci 1998;55:429–46.
- [17] de Haan JF, Bosma PB, Hovenier JW. The adding method for multiple scattering computations of polarized light. Astron Astrophys 1987;183:371–91.
- [18] Chowdhary J, Cairns B, Travis LD. Contribution of water-leaving radiances to multiangle, multispectral polarimetric observations over the open ocean: bio-optical model results for case 1 waters. Appl Opt 2006;45:5542–67.
- [19] Galassi M, Davies J, Theiler J, Gough B, Jungman B, Alken P, et al. GNU Scientific library reference manual, 3rd ed. Network Theory Ltd., ISBN: 0954612078.
- [20] Schulz FM, Stamnes K. Angular distribution of the Stokes vector in a plane-parallel vertically inhomogeneous medium in the vector discrete ordinate radiative transfer (VDISORT) model. J Quant Spectrosc Radiat Transfer 2000;65:609–20.
- [21] Yan B, Stamnes K. Fast yet accurate computation of the complete radiance distribution in the coupled atmosphere–ocean system. J Quant Spectrosc Radiat Transfer 2003;76:207–23.
- [22] Dave JV. Meaning of successive iteration of the auxiliary equation in the theory of radiative transfer. Astrophys J 1964;140:1292–303.
- [23] Ota Y, Higurashi A, Nakajima T, Yokota T. Matrix formulations of radiative transfer including the polarization effect in a coupled atmosphere–ocean system. J Quant Spectrosc Radiat Transfer 2010;111:878–94.
- [24] Zhai P, Hu Y, Trepte CR, Lucker PL. A vector radiative transfer model for coupled atmosphere and ocean systems based on successive order of scattering method. Opt Express 2009;17:2057–79.
- [25] Zhai P, Hu Y, Chowdhary J, Trepte CR, Lucker PL, Josset DB. A vector radiative transfer model for coupled atmosphere and ocean systems with a rough interface. J Quant Spectrosc Radiat Transfer 2010;111:1025–40.
- [26] Nakajima T, Tanaka M. Algorithms for radiative intensity calculations in moderately thick atmospheres using a truncation approximation. J Quant Spectrosc Radiat Transfer 1988;40:51–69.
- [27] Stamnes K, Tsay SC, Wiscombe W, Laszlo I. A general-purpose numerically stable computer code for discrete-ordinate-method radiative transfer in scattering and emitting layered media. DISORT Report v1.1. 2000.
- [28] Zhai P, Hu Y, Josset DB, Trepte CR, Lucker PL, Lin B. Exact first order scattering correction for vector radiative transfer in coupled atmosphere and ocean systems. Proc SPIE 2012;8364:83640A. <http://dx.doi.org/10.1117/12.920767>.
- [29] Kušćer I, Ribarić M. Matrix formalism in the theory of diffusion of light. Opt Acta 1959;6:42–51.
- [30] Siewert CE. On the phase matrix basic to the scattering of polarized light. Astron Astrophys 1982;109:195–200.
- [31] Hovenier JW, van der Mee CVM. Fundamental relationships relevant to the transfer of polarized light in a scattering atmosphere. Astron Astrophys 1983;128:1–16.
- [32] Kylling A, Stamnes K. Efficient yet accurate solution of the linear transport equation in the presence of internal sources: the exponential-linear-in depth approximation. J Comput Phys 1992;102:265–76.
- [33] Wiscombe WJ. The Delta-M method: rapid yet accurate radiative flux calculations for strongly asymmetric phase functions. J Atmos Sci 1977;34:1408–22.
- [34] Hu Y-X, Wielicki B, Lin B, Gibson G, Tsay S-C, Stamnes K, et al. δ -Fit: a fast and accurate treatment of particle scattering phase functions with weighted singular-value decomposition least-squares fitting. J Quant Spectrosc Radiat Transfer 2000;65:681–90.
- [35] Vestrucci P, Siewert CE. A numerical evaluation of an analytical representation of the components in Fourier decomposition of the phase matrix for the scattering of the polarized light. J Quant Spectrosc Radiat Transfer 1984;31:177–83.
- [36] Zhai P, Kattawar GW, Yang P. Impulse response solution to the three-dimensional vector radiative transfer equation in atmosphere-ocean systems. I. Monte Carlo method. Appl Opt 2008;47:1037–47.